The Canadian Mineralogist
Vol. 32, pp. 21-30 (1994)

A-SITE DISORDER IN SYNTHETIC FLUOR-EDENITE, A CRYSTAL-STRUCTURE STUDY

KATHLEEN F. BOSCHMANN, PETER C. BURNS, FRANK C. HAWTHORNE, MATI RAUDSEPP[1] AND ALLAN C. TURNOCK

Department of Geological Sciences, University of Manitoba, Winnipeg, Manitoba R3T 2N2

ABSTRACT

Large crystals of amphibole were synthesized by slow cooling of a bulk composition nominally that of end-member fluor-edenite. Electron-microprobe analysis shows the crystals to be zoned from a core composition close to end-member fluor-edenite to a rim composition close to the fluor-tremolite – fluor-pargasite join. The crystal structure of a fragment of average composition $Na_{0.912}(Ca_{1.926}Mg_{0.183})(Mg_{4.636}Al_{0.364})(Si_{6.507}Al_{1.493})O_{22}F_2$, *a* 9.821(1), *b* 17.934(4), *c* 5.282(1) Å, β 105.08(1)°, *V* 898.3(1) Å^3, *C2/m*, *Z* = 2, was refined to an *R* index of 2.9% for 1068 observed reflections collected with Mo*K*α X-radiation. Tetrahedrally coordinated Al is ordered at *T*(1), and octahedrally coordinated Al is ordered at *M*(2). The Na within the *A*-site cavity occupies both the *A*(*m*) and *A*(2) sites, and site-occupancy refinement shows Na to be equally partitioned between these two sites. This ordering scheme can be explained on the basis of local bond-valence requirements of the anions coordinating the *T*(1) site.

Keywords: amphibole, fluor-edenite, synthesis, crystal-structure refinement, ordering, electron-microprobe analyses.

SOMMAIRE

Nous avons réussi à synthétiser de gros cristaux d'amphibole en refroidissant lentement un mélange d'une composition globale égale à celle du pôle fluor-édenite. Une analyse à la microsonde électronique démontre que ces cristaux sont zonés, d'un coeur dont la composition est celle qui était prévue à une bordure dont la composition est proche de la solution solide fluor-trémolite – fluor-pargasite. La structure cristalline d'un fragment dont la composition moyenne serait $Na_{0.912}(Ca_{1.926}Mg_{0.183})(Mg_{4.636}Al_{0.364})(Si_{6.507}Al_{1.493})O_{22}F_2$, *a* 9.821(1), *b* 17.934(4), *c* 5.282(1) Å, β 105.08(1)°, *V* 898.3(1) Å^3, *C2/m*, *Z* = 2, a été affinée jusqu'à un résidu *R* de 2.9% en utilisant 1068 réflexions observées (rayonnement Mo*K*α). L'aluminium à coordinence tétraédrique occupe *T*(1), tandis que l'aluminium à coordinence octaédrique occupe *M*(2). Le Na du site *A* occupe les sites *A*(*m*) et *A*(2); l'affinement indique une répartition égale de l'atome Na entre ces deux sites. Ce schéma de mise en ordre découle des exigeances locales des valences de liaisons des anions en coordinence avec *T*(1).

(Traduit par la Rédaction)

Mots-clés: amphibole, fluor-édenite, synthèse, affinement de la structure cristalline, mise en ordre, données de microsonde électronique.

INTRODUCTION

There have been several attempts to synthesize edenite, ideally $NaCa_2Mg_5Si_7AlO_{22}(OH)_2$, but none of them have been very successful. Widmark (1974) and Hinrichsen & Schürmann (1977) both reported the synthesis of edenite, but the run yields were low, and Greenwood (1979) concluded that Widmark (1974) had synthesized overgrowths of tremolite on his seed crystals. Na *et al.* (1986) reported the coexistence of diopside and sodian phlogopite up to 3 kbar within the field of edenite – richterite (– tremolite) solid solution, and the results of Raudsepp *et al.* (1991) are broadly compatible with this. Thus the edenite end-member has not been synthesized as yet, and there is a strong possibility that it may not be stable. On the other hand, fluor-edenite has been synthesized on end-member composition (Graham & Navrotsky 1986). Raudsepp

[1]Present address: Department of Geological Sciences, University of British Columbia, Vancouver, British Columbia V6T 1Z4.

et al. (1991) attempted to synthesize large crystals of fluor-edenite by slow cooling of the nominal bulk composition from above the liquidus. Although electron-microprobe analysis showed that the crystals depart from the ideal fluor-edenite composition, the crystals were sufficiently large to characterize by crystal-structure refinement; the results are presented here.

EXPERIMENTAL

Synthesis

Forty mg of starting materials (fused silica glass, γ–Al_2O_3, CaF_2, Na_2CO_3, MgO) were sealed in a 4×23 mm Pt tube and placed in a conventional vertical quench-furnace. The run was held at 1240°C for 1 h and then cooled to 816°C over a period of 332 h. Further experimental details are given by Raudsepp *et al.* (1991).

In general, the run products were >90% amphibole, with minor forsterite, plagioclase, clinopyroxene and cristobalite. One particular run gave one large crystal (~10×3 mm) with minor fine-grained non-amphibole phases; this crystal was gently crushed to give more conveniently sized fragments, one of which was used in the present study.

Collection of the X-ray data

An irregular lath-like fragment of synthetic fluor-edenite was mounted on a Nicolet *R3m* automated four-circle diffractometer. Twenty-two reflections were centered using graphite-monochromated Mo$K\alpha$ X-radiation. The unit-cell dimensions (Table 1) were derived from the setting angles of twenty-two automatically aligned reflections by least-squares methods. A total of 1435 reflections was measured over the range ($3° < 2\theta < 60°$) with index ranges $0 \le h \le 13$, $0 \le k \le 25$, $-7 \le l \le 7$; reflections forbidden by the *C* face-centering were omitted. Two standard reflections were measured every fifty reflections; no significant changes in their net intensities occurred during data

TABLE 1. MISCELLANEOUS INFORMATION FOR FLUOR-EDENITE

Space group	*C2/m*	Crystal size (mm)	0.10x0.24x0.10
a (Å)	9.821(1)	Total Ref.	1435
b (Å)	17.934(4)	[I(obs) > 2.5σ(I)]	1068
c (Å)	5.282(1)		
β (°)	105.08(1)	Final *R*(obs)	2.9%
V (Å^3)	898.3(1)	Final *wR*(obs)	3.0%

Ideal cell contents: $2[NaCa_2Mg_5Si_7AlO_{22}F_2]$

Analyzed cell contents: $2[Na_{0.812}Ca_{1.929}Mg_{4.891}Al_{0.364}(Si_{6.507}Al_{1.492})O_{22}F_2]$

$R = \Sigma(|F_o|-|F_c|)/\Sigma|F_o|$

$wR = [\Sigma w(|F_o|-|F_c|)^2/\Sigma wF_o^2]^{1/2}$, $w = 1$

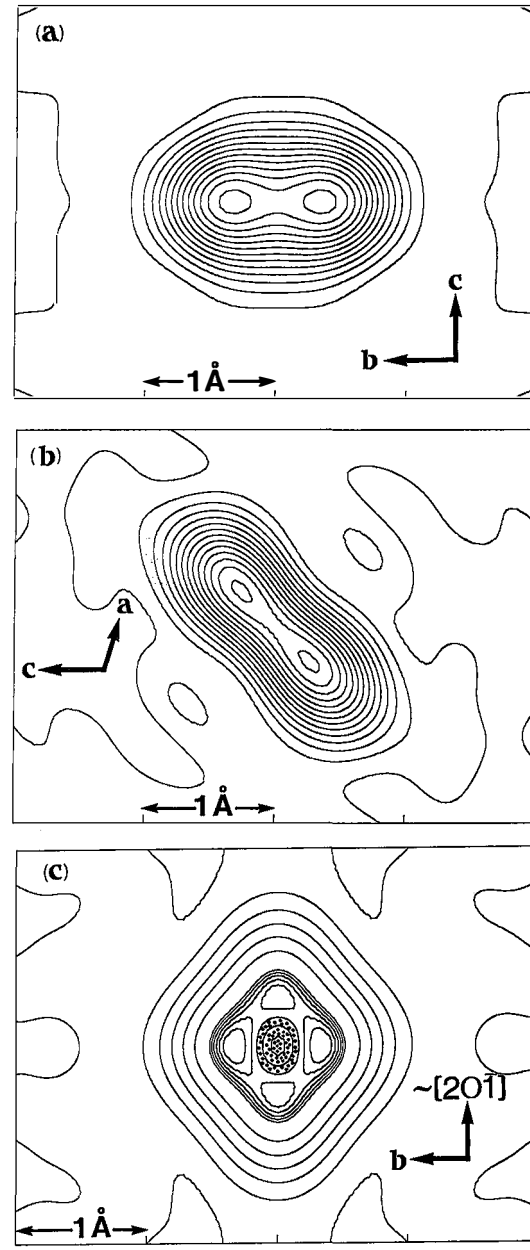

FIG. 1. Difference-Fourier sections through the central *A*(2/*m*) site with the A cation removed from the structural model: (a) (100) section at $x = 0$; (b) (010) section at $y = ½$; (c) section through the electron-density maxima on the 2-fold axis and in the mirror plane, approximately parallel to $(20\bar{1})$. In (a) and (b), the contour interval is 1 *e*/Å^3. In (c), the contour interval is 1 *e*/Å^3 below 6 *e*/Å^3, and 0.1 *e*/Å^3 above 6 *e*/Å^3; only this close contouring at high levels of density brings out the separate maxima on the 2-fold axis and within the mirror plane, and emphasizes the minimum at the central (0 ½ 0) position; this minimum is dot-shaded to distinguish it from the surrounding maxima.

collection. An empirical absorption-correction based on 396 psi-scan intensities was applied, reducing R (azimuthal) from 1.3 to 0.9%. The data were corrected for Lorentz, polarization and background effects, and reduced to structure factors; of the 1435 reflections measured, there were 1068 unique observed [$I \geq 2.5\sigma(I)$] reflections.

Structure refinement

Scattering curves for neutral atoms, together with anomalous dispersion corrections, were taken from Cromer & Mann (1968) and Cromer & Liberman (1970), respectively. The Siemens SHELXTL PLUS (PC Version) system of programs was used throughout this study. R indices are of the form given in Table 1, and are expressed as percentages.

Least-squares refinement of the structure in the space group $C2/m$, with starting parameters taken from Hawthorne (1983) and an isotropic displacement model, converged to an R index of 5.1%. Conversion to an anisotropic displacement model, together with the refinement of all parameters, converged to a R index of 3.2% and a wR index of 3.3%. A model with weighted structure-factors and an isotropic extinction correction was tried but did not lead to any improvement in the refinement. As is usual for amphiboles with a full A-site, the $A(2/m)$ displacement factor was found to be very large ($U \approx 0.16$), indicative of significant positional disorder in the cavity surrounding the A site (Hawthorne & Grundy 1972). This feature is of considerable interest in the present case because of the fairly simple composition of the amphibole. The A cation was removed from the refinement model, and a series of difference-Fourier maps were calculated through the A site (Fig. 1). The (100) section at $x = 0$ shows significant displacement of the maximum electron-density along the 2-fold axis (Fig. 1a) parallel to [010], the $A(2)$ position. The (010) section at $y = \frac{1}{2}$ shows significant displacement of the maximum electron-density within the mirror plane (Fig. 1b), the $A(m)$ site. In order to assess the relative electron-densities at these different sites, a difference-Fourier map was calculated in the plane of the maximum electron-density through the central A-site (Fig. 1c). Note the variability in contour intervals in this section: above 6 e/Å^3, the interval is 0.1 e, whereas below 6 e/Å^3, it is 1.0 e; this was done to emphasize the relative electron-densities at the $A(2)$ and $A(m)$ positions, and to show that there is an electron-density minimum (dotted) at the central $A(2/m)$ position. Figure 1c indicates that there is very slightly less electron-density at $A(m)$ relative to $A(2)$, but the difference is very small, and thus the electron-densities are approximately the same.

The coordinates of the $A(m)$ and $A(2)$ positions were taken from the difference-Fourier maps, and Na was initially split equally between the two sites; isotropic displacement factors were used for the $A(m)$ and $A(2)$ positions, and were fixed at 0.02 for each site. Full-matrix least-squares refinement converged to an R index of 2.9% and an wR index of 3.0%. Final positional parameters and equivalent isotropic displacement parameters are given in Table 2, anisotropic displacement parameters in Table 3 and

TABLE 2. FINAL POSITIONAL PARAMETERS AND EQUIVALENT ISOTROPIC DISPLACEMENT PARAMETERS (Å^{2}x10^4) FOR FLUOR-EDENITE

	x	y	z	$U_{equiv.}$
$T(1)$	0.28176(8)	0.08479(4)	0.3025(2)	82(2)
$T(2)$	0.29057(8)	0.17251(4)	0.8113(2)	71(2)
$M(1)$	0	0.08902(7)	1/2	66(4)
$M(2)$	0	0.17547(7)	0	64(4)
$M(3)$	0	0	0	66(6)
$M(4)$	0	0.27854(5)	1/2	115(3)
$A(m)$**	0.0415(9)	1/2	0.0953(20)	200*
$A(2)$**	0	0.4765(5)	0	200*
$O(1)$	0.1084(2)	0.0860(1)	0.2182(4)	97(5)
$O(2)$	0.1191(2)	0.1714(1)	0.7312(4)	91(5)
$O(3)$	0.1044(3)	0	0.7133(5)	107(7)
$O(4)$	0.3656(2)	0.2504(1)	0.7884(4)	115(6)
$O(5)$	0.3511(2)	0.1391(1)	0.1108(4)	128(6)
$O(6)$	0.3462(2)	0.1164(1)	0.6075(4)	133(6)
$O(7)$	0.3448(3)	0	0.2784(7)	129(8)

* fixed during refinement
** $A(m)$ and $A(2)$ populations are 0.24(1) and 0.25(1) Na, respectively.

TABLE 3. ANISOTROPIC DISPLACEMENT PARAMETERS (Å^{2}x10^4) FOR FLUOR-EDENITE

	U_{11}	U_{22}	U_{33}	U_{23}	U_{13}	U_{12}
$T(1)$	78(4)	84(3)	80(3)	-2(3)	14(3)	-3(2)
$T(2)$	66(3)	79(3)	67(3)	2(3)	14(2)	-3(3)
$M(1)$	75(7)	69(6)	56(7)	0	20(5)	0
$M(2)$	61(6)	70(6)	62(7)	0	19(4)	0
$M(3)$	68(9)	57(9)	68(9)	0	7(6)	0
$M(4)$	134(4)	110(4)	120(4)	0	67(3)	0
$O(1)$	81(8)	122(9)	89(9)	-13(7)	24(7)	-13(7)
$O(2)$	83(8)	90(8)	91(5)	7(7)	12(7)	2(7)
$O(3)$	106(11)	110(10)	111(11)	0	40(9)	0
$O(4)$	140(9)	94(8)	119(9)	-3(7)	46(8)	-26(7)
$O(5)$	111(9)	157(9)	107(9)	43(8)	13(7)	-7(7)
$O(6)$	102(9)	158(10)	136(10)	-52(8)	28(8)	13(7)
$O(7)$	117(13)	107(12)	174(14)	0	56(11)	0

TABLE 4. SELECTED INTERATOMIC DISTANCES (Å) AND ANGLES (°) FOR FLUOR-EDENITE

T(1)-*O*(1)	1.644(2)	*M*(2)-*O*(1) x2	2.097(2)
T(1)-*O*(5)	1.673(3)	*M*(2)-*O*(2)b x2	2.062(2)
T(1)-*O*(6)	1.670(2)	*M*(2)-*O*(4)c x2	1.998(2)
T(1)-*O*(7)	1.659(2)	<*M*(2)-*O*>	2.053
<*T*(1)-*O*>	1.661		
		M(3)-*O*(1) x4	2.050(2)
T(2)-*O*(2)	1.626(2)	*M*(3)-*O*(3)a x2	2.037(3)
T(2)-*O*(4)	1.598(2)	<*M*(3)-*O*>	2.045
T(2)-*O*(6)	1.666(3)		
T(2)-*O*(5)a	1.651(2)	*M*(4)-*O*(2) x2	2.410(2)
<*T*(2)-*O*>	1.635	*M*(4)-*O*(4)c x2	2.319(2)
		M(4)-*O*(5)c x2	2.642(2)
M(1)-*O*(1) x2	2.044(2)	*M*(4)-*O*(6)c x2	2.569(2)
M(1)-*O*(2) x2	2.074(2)	<*M*(4)-*O*>	2.485
M(1)-*O*(3) x2	2.066(2)		
<*M*(1)-*O*>	2.061	*A*-*O*(5) x4	3.024(2)
		A-*O*(6) x4	3.051(2)
		A-*O*(7) x4	2.380(4)
		<*A*-*O*>	2.906
A(*m*)-*O*(5) x2	3.020(7)	*A*(2)-*O*(5) x2	2.687(7)
A(*m*)-*O*(5) x2	3.131(6)	*A*(2)-*O*(5) x2	3.382(8)
A(*m*)-*O*(6) x2	2.672(6)	*A*(2)-*O*(6) x2	2.779(6)
A(*m*)-*O*(6) x2	3.479(7)	*A*(2)-*O*(6) x2	3.354(7)
A(*m*)-*O*(7)	2.375(11)	*A*(2)-*O*(7) x2	2.415(4)
A(*m*)-*O*(7)	2.509(12)	*A*(2)-*O*(7) x2	3.473(6)
A(*m*)-*O*(7)	3.204(10)		
A(*m*)-*O*(7)	4.244(11)		
T(1) tetrahedron			
O(1)-*O*(5)	2.759(3)	*O*(1)-*T*(1)-*O*(5)	112.6(1)
O(1)-*O*(6)	2.735(3)	*O*(1)-*T*(1)-*O*(6)	111.3(1)
O(1)-*O*(7)	2.734(3)	*O*(1)-*T*(1)-*O*(7)	111.8(1)
O(5)-*O*(6)	2.669(3)	*O*(5)-*T*(1)-*O*(6)	106.0(1)
O(5)-*O*(7)	2.654(3)	*O*(5)-*T*(1)-*O*(7)	105.6(2)
O(6)-*O*(7)	2.714(3)	*O*(6)-*T*(1)-*O*(7)	109.3(1)
<*O*-*O*>	2.711	<*O*-*T*(1)-*O*>	109.4

TABLE 4. (cont.)

T(2) tetrahedron			
O(2)-*O*(4)	2.753(3)	*O*(2)-*T*(2)-*O*(4)	117.3(1)
O(2)-*O*(6)	2.670(3)	*O*(2)-*T*(2)-*O*(6)	108.5(1)
O(2)-*O*(5)a	2.678(3)	*O*(2)-*T*(2)-*O*(5)a	109.6(1)
O(4)-*O*(6)	2.574(3)	*O*(4)-*T*(2)-*O*(6)	104.1(1)
O(4)-*O*(5)a	2.651(3)	*O*(4)-*T*(2)-*O*(5)a	109.3(1)
O(6)-*O*(5)a	2.676(3)	*O*(6)-*T*(2)-*O*(5)a	107.6(1)
<*O*-*O*>	2.667	<*O*-*T*(2)-*O*>	109.4
M(1) octahedron			
O(1)-*O*(2) x2	3.090(3)	*O*(1)-*M*(1)-*O*(2) x2	97.3(1)
O(1)-*O*(3) x2	3.047(3)	*O*(1)-*M*(1)-*O*(3) x2	95.7(1)
O(1)-*O*(2)d x2	2.780(3)	*O*(1)-*M*(1)-*O*(2)d x2	84.9(1)
O(1)-*O*(3)d x2	2.696(3)	*O*(1)-*M*(1)-*O*(3)d x2	82.0(1)
O(2)-*O*(3) x2	3.077(2)	*O*(2)-*M*(1)-*O*(3) x2	96.0(1)
O(2)-*O*(2)d	2.910(4)	*O*(2)-*M*(1)-*O*(2)d	89.1(1)
O(3)-*O*(3)d	2.624(5)	*O*(3)-*M*(1)-*O*(3)d	78.9(1)
<*O*-*O*>	2.909	<*O*-*M*(1)-*O*>	89.98
M(2) octahedron			
O(1)-*O*(2)b x2	3.019(3)	*O*(1)-*M*(2)-*O*(2)b x2	93.1(1)
O(1)-*O*(2)d x2	2.780(3)	*O*(1)-*M*(2)-*O*(2)d x2	83.8(1)
O(1)-*O*(4)c x2	2.946(3)	*O*(1)-*M*(2)-*O*(4)c x2	92.0(1)
O(2)d-*O*(4)c x2	2.941(3)	*O*(2)d-*M*(2)-*O*(4)c x2	92.8(1)
O(2)d-*O*(4)f x2	2.869(3)	*O*(2)d-*M*(2)-*O*(4)f x2	89.9(1)
O(1)-*O*(1)e	2.702(4)	*O*(1)-*M*(2)-*O*(1)e	80.2(1)
O(4)c-*O*(4)f	2.982(4)	*O*(4)c-*M*(2)-*O*(4)f	96.5(1)
<*O*-*O*>	2.900	<*O*-*M*(2)-*O*>	89.98
M(3) octahedron			
O(1)-*O*(3)a x4	3.070(3)	*O*(1)-*M*(3)-*O*(3)a x4	97.4(1)
O(1)-*O*(3)e x4	2.696(3)	*O*(1)-*M*(3)-*O*(3)e x4	82.6(1)
O(1)-*O*(1)g x2	2.702(4)	*O*(1)-*M*(3)-*O*(1)g x2	82.4(1)
O(1)-*O*(1)h x2	3.084(4)	*O*(1)-*M*(3)-*O*(1)h x2	97.6(1)
<*O*-*O*>	2.886	<*O*-*M*(3)-*O*>	90.00
M(4) polyhadron			
O(2)-*O*(2)e	2.910(4)	*O*(2)-*M*(4)-*O*(2)e	74.3(1)
O(2)-*O*(4)c x2	3.121(3)	*O*(2)-*M*(4)-*O*(4)c x2	82.6(1)
O(2)-*O*(4)i x2	2.941(3)	*O*(2)-*M*(4)-*O*(4)i x2	76.9(1)
O(2)-*O*(5)c x2	3.494(3)	*O*(2)-*M*(4)-*O*(5)c x2	87.4(1)
O(4)c-*O*(5)i x2	3.352(3)	*O*(4)c-*M*(4)-*O*(5)i x2	84.7(1)
O(4)c-*O*(6)c x2	2.574(3)	*O*(4)c-*M*(4)-*O*(5)c x2	63.3(1)
O(5)c-*O*(6)c x2	2.669(3)	*O*(5)c-*M*(4)-*O*(6)c x2	61.6(1)
O(5)c-*O*(6)j x2	2.985(3)	*O*(5)c-*M*(4)-*O*(6)j x2	69.9(1)
O(6)c-*O*(6)j	3.493(5)	*O*(6)c-*M*(4)-*O*(6)j	85.6(1)
<*O*-*O*>	3.042	<*O*-*M*(4)-*O*>	75.79

a = *x*, *y*, *z*+1; b = *x*, *y*, *z*-1; c = ½-*x*, ½-*y*, 1-*z*; d = -*x*, *y*, 1-*z*; e = -*x*, *y*, 1-*z*; f = *x*-½, ½-*y*, *z*-1; g = -*x*, *y*, -*z*; h = *x*, -*y*, *z*; i = *x*-½, ½-*y*, *z*; j = *x*+½, *y*-½, *z*

selected bond-distances, angles and polyhedral edge-lengths are given in Table 4. Observed and calculated structure-factors are available from the Depository of Unpublished Data, CISTI, National Research Council of Canada, Ottawa, Ontario K1A 0S2.

Electron-microprobe analysis

Following collection of the X-ray intensity data, the crystal was mounted in epoxy, polished, carbon-coated and analyzed by electron microprobe. The analyses were done on a fully automated Cameca SX–50 according to the procedure of Raudsepp *et al.* (1991). As a control on accuracy, diopside and forsterite of known compositions were analyzed at the same time; these showed close agreement with the nominal compositions. Ten points were analyzed on the crystal; the results of individual analyses are given in Table 5, as significant zoning is present in the crystal. The average composition was calculated from the distribution of compositions over the crystal, and this also is given in Table 5. As the chemical composition of this crystal is a very important factor in this work, we repeated the electron-microprobe analysis (a different set of 10 points) several months later, and bracketed the analysis of fluor-edenite by analysis of a sample of olivine and one of diopside of known compositions. The latter compositions determined here were found to be accurate, supporting the results for fluor-edenite;

TABLE 5. RESULTS OF ELECTRON-MICROPROBE ANALYSIS OF SYNTHETIC 'FLUOR-EDENITE'

	Min.*	Max.*	Mean*	Mean†	End-member
SiO_2	48.78	44.57	46.76	47.22	50.16
Al_2O_3	8.98	13.35	11.32	11.00	6.08
MgO	24.04	22.87	23.23	23.16	24.06
CaO	12.46	13.11	12.92	13.03	13.38
Na_2O	3.58	3.17	3.38	3.41	3.70
F	5.14	5.23	5.08	5.01	4.53
O≡F	-2.16	-2.20	-2.14	-2.11	-1.91
Total**	100.81	100.10	100.55	100.72	100.00
Si	6.755	6.225	6.507	6.555	7.000
Al	1.245	1.775	1.493	1.445	1.000
ΣT	8.000	8.000	8.000	8.000	8.000
Al	0.221	0.432	0.364	0.355	—
Mg	4.963	4.783	4.819	4.793	5.000
ΣC	5.184	5.215	5.183	5.148	5.000
Mg	0.208	0.215	0.183	0.148	—
Ca	1.849	1.970	1.926	1.938	2.000
	2.057	2.185	2.109	2.086	2.000
Na	0.961	0.862	0.912	0.918	1.000

* from first set of analytical results;
† from second set of analytical results;
** the totals are a trifle high; using the ideal F-content reduces them by ~0.5 wt%.

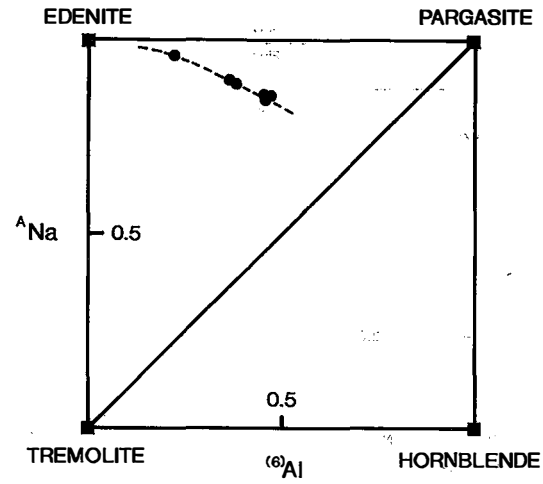

FIG. 2. Variation in composition with regard to *A*-site Na and [6]-coordinated Al across the crystal used for the collection of X-ray intensity data.

the latter are similar to the values obtained previously (Table 5), and also suggested that the mean composition is fairly representative of the whole crystal.

Unit formulae were calculated on the basis of 23 equivalent oxygen atoms. The analyzed F values (~5.1 wt%) are slightly higher than the nominal value (4.5 wt%); as the structure cannot accommodate F in excess of the ideal amount, the analyzed values are thus a little high (albeit equal to the nominal value within two standard deviations).

DISCUSSION

Although the ideal composition of the synthesized crystal is end-member fluor-edenite, both the electron-microprobe analyses and the X-ray data show that it deviates significantly from this composition. The compositional variation in the fragment used for the X-ray work (Fig. 2) lies within the compositional field of edenite. The spatial distribution of compositions shows that the original crystal had a core close to (or perhaps on) the ideal end-member composition, becoming richer in tschermakite component (*i.e.*, moving toward the tremolite – pargasite join) toward the edge of the crystal. As the crystal grew during slow cooling, the observed variation in composition indicates that the composition of the stable amphibole in this system is very sensitive to the temperature of crystallization.

The site populations in this crystal are of particular interest. Firstly, the composition is simpler than most natural amphiboles, and there should be close agreement with established site-population and stereochemical relations. Secondly, this composition provides an opportunity to examine *A*-cation positional disorder (Hawthorne & Grundy 1972) for a simple *A*-site chemistry with $^{[4]}$Al present and F at the *O*(3) position.

The *C*- and *T*-group cations are Mg, Al and Si, with atomic numbers of 12, 13 and 14, respectively. These scatter X rays in a very similar fashion, and hence we cannot use site-scattering refinement to derive site populations. However, these cations are of very different sizes ($^{[6]}$Mg = 0.72, $^{[6]}$Al = 0.535, $^{[4]}$Al = 0.39, $^{[4]}$Si = 0.26 Å; Shannon 1976) and thus the mean bond-lengths can be used to derive the site populations.

T(1) and T(2) sites

For an amphibole of this composition, $^{[4]}$Al is expected to order at *T*(1). In synthetic fluor-amphiboles with no $^{[4]}$Al, $\langle T(2)\text{–O}\rangle \approx 1.632$ Å (Table 6); hence *T*(2) = Si in fluor-edenite. On the other hand, the observed $\langle T(1)\text{–O}\rangle$ distance of 1.661 Å in fluor-edenite is much larger than the mean $\langle T(1)\text{–O}\rangle$ value for complete Si occupancy of *T*(1): 1.620 Å (Table 6); consequently, $^{[4]}$Al is completely ordered at *T*(1). Hawthorne & Grundy (1977) and

TABLE 6. SELECTED MEAN BOND-LENGTHS (Å) IN SYNTHETIC FLUOR-AMPHIBOLES

	Fluor-richterite	Fluor-tremolite	K-fluor-richterite	Fluor-edenite
T(1)	Si	Si	Si	(Si,Al)
<*T*(1)-*O*>	1.622	1.620	1.619	1.661
T(2)	Si	Si	Si	Si
<*T*(2)-*O*>	1.632	1.629	1.634	1.635
M(1)	Mg	Mg	Mg	Mg
<*M*(1)-*O*>	2.050	2.054	2.052	2.061
M(2)	Mg	Mg	Mg	(Mg,Al)
<*M*(2)-*O*>	2.087	2.082	2.088	2.053
M(3)	Mg	Mg	Mg	Mg
<*M*(3)-*O*>	2.041	2.040	2.044	2.045
M(4)	$Na_{1/2}Ca_{1/2}$	Ca	$Na_{1/2}Ca_{1/2}$	Ca
<*M*(4)-*O*>[6]	2.544	2.459	2.555	2.485
Ref.	(1)	(2)	(1)	(3)

Refs: (1) Cameron et al. (1983); (2) Cameron & Gibbs (1973); (3) this study.

Bocchio *et al.* (1978) both gave predictive curves for the amount of $^{[4]}$Al in amphibole based on <*T*–O> distances; the predicted values are 1.40 and 1.56 Al pfu (per formula unit), respectively, bracketing the observed value of 1.49 Al pfu.

The M(1) and M(3) sites

The *C*-group cations occupy these sites, and the composition of the crystal constrains the site populations to be (Mg, Al). Inspection of Table 6 shows the *M*(1) and *M*(3) sites to be completely occupied by Mg. The <*M*(1)–O> distance of 2.061 Å is slightly larger than the average <*M*(1)–O> distance of 2.052 Å for the other synthetic fluor-amphiboles (Table 6). As the only other possible constituent of this site is much smaller than Mg, this means that the *M*(1) site must be occupied completely by Mg. The <*M*(3)–O> distance of 2.045 Å is statistically equal to the average <*M*(3)–O> value of 2.042 Å for the other synthetic fluor-amphiboles, and hence *M*(3) must be completely occupied by Mg.

The M(2) site

The expected <*M*(2)–O> distance for complete Mg occupancy of *M*(2) is 2.086 Å, significantly larger than the observed <*M*(2)–O> value of 2.053 Å for fluor-edenite. This indicates occupancy of *M*(2) by Al as well as Mg. Assigning all of the $^{[6]}$Al (Table 5) to the *M*(2) site, we can calculate the expected <*M*(2)–O> distance from the curve of Hawthorne (1983) relating <*M*(2)–O> distance to constituent cation radius. A value of 2.055 Å is obtained, in good agreement with the observed value of 2.053 Å. Ungaretti *et al.* (1981) and Hawthorne (1983) have published "ideal" <*M*–O> distances for specific cations; using these values, (binary) site populations can be derived algebraically from observed mean bond-lengths. These procedures give *M*(2) occupancies of $(Mg_{0.832}Al_{0.168})$ and $(Mg_{0.798}Al_{0.202})$, respectively, both in close agreement with the electron-microprobe values of $(Mg_{0.818}Al_{0.182})$.

M(4) site

The formula unit calculated from the results of the electron-microprobe analysis has a *C*-group cation excess of Mg (0.18 apfu, Table 5). Where calcic, sodic–calcic and alkali amphiboles contain significant amounts of *B*-group cations (Fe^{2+},Mn,Mg), careful structure-refinement has shown the presence of significant electron-density at *M*(4′), a site very close to *M*(4) but displaced along the 2-fold axis toward the octahedral strip (Oberti *et al.* 1992). Difference-Fourier maps of fluor-edenite, calculated with the *M*(4) cation removed from the model, show no sign of an *M*(4′) site, and neither did analogous Fourier maps. An *M*(4′) site was inserted into the refinement procedure, but refined to zero Mg occupancy. Refinement of the total scattering at the *M*(4) site gave a value of 38.96 epfu (electrons per formula unit), supporting the Ca content of the unit formula (~1.93 apfu) derived by electron-microprobe analysis. Thus there is a deficiency in scattering relative to occupancy of *M*(4) by 2.0 Ca apfu, but another (displaced) site is not apparent. This gives us three possibilities: (1) the balance of the *M*(4) occupancy (~0.10 apfu) is Mg; in this case, Mg must occupy the *M*(4) site rather than the *M*(4′) site, or we would be able to distinguish the *M*(4′) site. (2) The balance of the *M*(4) occupancy is Na; in this case, one would expect Na to occupy the *M*(4) site (and hence there would be no scattering from an *M*(4′) site. (3) All Mg occurs at *M*(4), and a small amount of Ca occurs at the *A* site.

If significant Mg were to occur at the *A* site, this should be visible as a separate site [probably a *separate A*(2) position] because of the short Mg–O bonds required; no such site was visible in difference-Fourier maps. Thus it seems reasonable to adopt that model with the minimum amount of Mg at the *A* site [model (3)]. The problem with this model is that there is no *M*(4′) site to accept the Mg; possibly the Mg assumes a more disordered position than Fe^{2+} or Mn^{2+} if it is a *B*-group cation (in calcic amphiboles). This model is not entirely satisfactory, but we consider it to be slightly better than the other two possibilities.

The observed <*M*(4)–O> distance of 2.485 Å in fluor-edenite is significantly larger than that in fluor-tremolite, 2.459 Å (Table 6), in which *M*(4) also is occupied by Ca. However, this difference is inducti-

vely caused by stereochemical differences in the rest of the structure (Hawthorne 1983), particularly the presence of the *A* cation in fluor-edenite. Comparison with the mean *M*(4) bond-length in the pargasite of Bocchio *et al.* (1978), where *M*(4) ≈ Ca and *A* ≈ (Na,□), show these two structures to be very similar in this respect.

The A(m) and A(2) sites

Much work has been done on this particular aspect of amphibole structure. Heritsch (1955) refined the structure of an edenitic hornblende and noted the *A*-site Na displaced along the 2-fold axis at the *A*(2) site. Prewitt (1963) and Gibbs & Prewitt (1968) reported Na occupancy of the *A*(2) site in synthetic $Na_2H_2Co_5Si_8O_{22}(OH)_2$ and Na occupancy of *A*(*m*) in synthetic $Na_2H_2Mg_5Si_8O_{22}F_2$, and Gibbs (1966) suggested that *A*(2) or *A*(*m*) is occupied if *O*(3) is OH or F, respectively. Papike *et al.* (1969) reported strong ordering at the *A*(*m*) site in potassian titanian magnesio-hastingsite and potassian magnesio-kataphorite; in both these crystals, the dominant *A* cation is K. Hawthorne & Grundy (1972, 1973a,b) proposed that positional disorder occurs between the *A*(2) and *A*(*m*) sites. Hawthorne & Grundy (1978) tested numerous models for a potassian ferri-taramite, and concluded that the best model involves disorder over *A*(2) and *A*(*m*), with ordering of K at *A*(*m*) and ordering of Na at *A*(2). Ungaretti (1980) and Ungaretti *et al.* (1981) documented *A*-site disorder in a wide range of natural amphiboles; they showed that K does order at the *A*(*m*) site, but that Na occurs both at the *A*(*m*) and *A*(2) sites. Cameron *et al.* (1983) refined the structures of potassian fluor-richterite and fluor-richterite. They showed that K orders at *A*(*m*), but proposed that Na occupies the general position *A*(1) (*i.e.*, Wyckoff position 8*j* in C2/*m*). Thus it seems well established that K orders at *A*(*m*), and that Na can be disordered over the *A*(*m*) and *A*(2) positions, and possibly also occupies the *A*(1) position.

Bond-valence arguments

There have been many suggestions as to the important factors affecting *A*-site ordering in amphiboles. From the above discussion, it is obvious that the most important feature is the identity of the cation: K behaves differently from Na. Hawthorne & Grundy (1978) and Hawthorne (1983) examined this aspect of the problem with bond-valence theory (Brown & Shannon 1973, Brown 1981). For a variety of amphiboles, they showed that if K is placed at *A*(2/*m*), there is a bond-valence excess at the cation, whereas if Na is placed at *A*(2/*m*), there is a bond-valence deficiency at the cation. This suggests that K and Na will behave differently with regard to *A*-site ordering. The bond-valence excess at K vanishes if K occupies the *A*(*m*) site, whereas the excess is still present if K resides at *A*(2); thus K will order at the *A*(*m*) site because it is only at this site that its bond-valence requirements are satisfied. The situation is less clear for Na. There is still significant bond-valence deficiency at the cation if Na occurs at *A*(2) [bond-valence sums average ~0.86 v.u.] or at *A*(*m*), and it is not feasible to make predictions on this basis. Possibly this reflects the much more complex behavior of Na relative to K at the *A* site.

The complex behavior of Na is presumably related to the local next-nearest-neighbor cation arrangements, as these will produce local variations in the bond-valence incident to the anions surrounding the *A*(2) position, together with associated bond-length relaxations. Factors that will be important in this respect include the $^{[4]}$Al content and its ordering over *T*(1) and *T*(2) (Hawthorne & Grundy 1977), content and ordering of tri- and tetravalent cations in the octahedral strip (Hawthorne & Grundy 1973a), the identity of the *O*(3) anion (Gibbs & Prewitt 1968), and the nature of the *B* cations [*i.e.*, Na or Ca at the surrounding *M*(4) sites (Cameron *et al.* 1983)]. However, most natural amphiboles have too complicated a bulk composition to be able to untangle the competing influences of these possible factors, and the relative importance of these effects is still unresolved.

Energetic considerations

Docka *et al.* (1987) have taken a different approach to this problem; they modeled the various possibilities for local ordering with techniques of structure-energy minimization. Their calculations suggest that if a local charge-configuration at the second-nearest-neighbor cation sites around the *A* site obeys a symmetry element (or combination of symmetry elements), the minimum energy position for the *A* cation lies on that symmetry element (or combination of symmetry elements). If the local charge arrangement is asymmetrical, the minimum-energy position lies on the general position *A*(1) (8*j*). However, calculations for K show the minimum-energy position to lie on or close to the mirror plane. This is compatible with the observation of K always at the *A*(*m*) position, as it is probable that neither the calculation nor the structure refinements are sensitive to the very small displacements that constitute the difference between the two sets of results. The situation for Na is more involved. The minimum-energy positions for asymmetrical arrangements of charges lie at the *A*(1) position, but closer to *A*(2) than *A*(*m*). In some cases, the distance between the energy minimum and the *A*(2) position is below the resolution of X rays, and *A*(2) occupancy would be observed even if the *A*(1) positions were occupied. In other instances, this is not the case, and *A*(1) occupancy should be observable by structure refinement if the calculations are accurate.

Results for fluor-edenite

The difference-Fourier maps (Fig. 1) show that $A(m)$ and $A(2)$ are both occupied; there is a minimum at the $A(2/m)$ position and a saddle-point at the $A(1)$ position. Thus the $A(1)$ position is not occupied within the resolution of the X-ray method. Furthermore, site-scattering refinement shows Na (+ minor Ca) to be equally partitioned between the $A(2)$ and $A(m)$ sites. Firstly, we can say that the ordering is not the result of (OH,F) substitution at $O(3)$ or (Ca,Na) substitution at $M(4)$, as these do not occur for this specific composition. Similarly, the suggestion of Hawthorne & Grundy (1978) that K orders at $A(m)$ and Na orders at $A(2)$ is not correct. From the above discussion of site populations in the structure, the only possible factors affecting the local arrangement of charges are (Al,Si) disorder at $T(1)$ and (Al,Mg) disorder at $M(2)$. Docka *et al.* (1987) found the minimum-energy position for the case of Al occupancy of $T(1)$ at the $A(1)$ position, with an $A(1)$–$A(1)$ displacement of ~0.6 Å across the 2-fold axis. This is not compatible with the results for this fluor-edenite (Fig. 1, Table 2). Either the small amount of $^{[6]}$Al has drastically altered the general energetic situation here, or the omission of local relaxations associated with the different arrangements of charges has adversely affected the calculations.

It is difficult to reconcile the (exactly) equal partitioning of Na between the $A(2)$ and $A(m)$ sites with the intermediate (*i.e.*, non-end-member) composition of the crystal. In fact, it seems reasonable to conclude that the ordering must be fairly independent of small changes in bulk composition in this particular case. The key feature here is the recognition that although the A cavity is surrounded by eight equivalent $T(1)$ tetrahedra, these tetrahedra are *not* all equivalent through the point-symmetry operations at the $A(2/m)$ position. This is illustrated diagrammatically in Figure 3. Consider first the A site on the left of the figure. The adjoining $T(1)$ sites fall into two sets, $T(1)'$ and $T(1)''$, that are distinct with regard to the point symmetry at the $A(2/m)$ position. Thus when considering energy calculations based on a single cluster centered on one $A(2/m)$ site, *it is necessary to treat substitutions at the $T(1)'$ and $T(1)''$ sites as distinct.*

Inspection of Table 4 shows that $A(2)$ has short bonds to O(5) and O(7), whereas $A(m)$ has short bonds to O(6). Adjacent A cavities are connected, and each $T(1)$ tetrahedron is adjacent to two cavities (Fig. 3). This immediately suggests a reason for the equally occupied $A(2)$ and $A(m)$ sites in the fluor-edenite crystal examined here. If a specific $T(1)$ site is occupied by Al, the adjacent O(5), O(6) and O(7) anions have a significant bond-valence deficiency. In one adjacent A-cavity, Na occupies the $A(m)$ position and increases the bond-valence incident to the associated O(6) anion. In the other adjacent A-cavity, Na occupies the $A(2)$ position and increases the bond-valence incident to the associated O(5) and O(7) anions. Each bridging anion coordinated to $T(1)$ thus has additional incident bond-valence from this local arrangement, and will cause equal occupancy of the $A(m)$ and $A(2)$ positions. This arrangement may propagate along the chain of A cavities parallel to the c axis to form an ordered arrangement, but there is no way that this arrangement can be propagated to adjacent chains of A cavities, and thus long-range $C2/m$ symmetry with the usual cell of amphibole is preserved.

The argument advanced above for equal occupancy

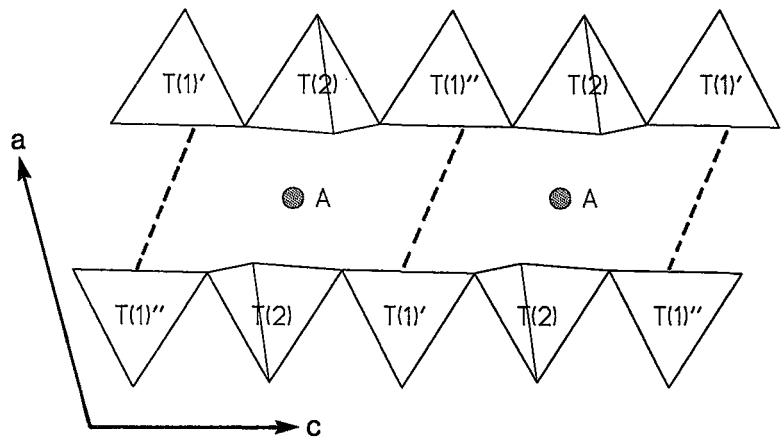

FIG. 3. The A-site cavity and surrounding anions viewed down [010]. The $T(1)'$ and $T(1)''$ tetrahedra form two sets that are *not* related by the point symmetry at the A position; a single $T(1)$ tetrahedron has different relationships to the central A-position in each cavity. The broken lines show the limits of each A cavity.

of the $A(m)$ and $A(2)$ positions is general and suggests that such a configuration should be the usual case in amphiboles. However, the experimental situation is less clear, as the assignment of A-site populations is commonly complicated by the presence of K, and the argument may need to be modified if other ordering schemes [*e.g.*, Al at $M(2)$, Na at $M(4)$, OH at O(3)] also are present; these factors are currently being examined in detail by Oberti *et al.* (work in progress).

Conclusions

1. The compositional results suggest that the deviation of amphibole composition from nominal in the fluor-edenite system is a function of the temperature of crystallization.
2. Tetrahedrally coordinated Al is ordered at $T(1)$ in this synthetic fluor-edenite.
3. Octahedrally coordinated Al is ordered at $M(2)$.
4. ^{A}Na is equally partitioned between the $A(m)$ and $A(2)$ sites in this synthetic fluor-edenite.
5. The equal occupancy of the $A(m)$ and $A(2)$ sites by Na can be explained on the basis of local bond-valence requirements of the anions coordinating the $T(1)$ site.

Acknowledgements

We thank Luciano Ungaretti and an anonymous reviewer for comments that materially improved this paper. Financial support was provided by the Natural Sciences and Engineering Research Council of Canada *via* a Post-graduate Fellowship to PCB and Operating, Equipment and Infrastructure Grants to FCH.

References

Bocchio, R., Ungaretti, L. & Rossi, G. (1978): Crystal chemical study of eclogitic amphiboles from Alpe Arami, Lepontine Alps, southern Switzerland. *Soc. Ital. Mineral. Petrol. Rend.* **34**, 453-470.

Brown, I.D. (1981): The bond-valence method: an empirical approach to chemical structure and bonding. *In* Structure and Bonding in Crystals II (M. O'Keeffe & A. Navrotsky, eds.). Academic Press, New York (1-30).

——— & Shannon, R.D. (1973): Empirical bond-strenth – bond-length curves for oxides. *Acta Crystallogr.* **A29**, 266-282.

Cameron, M. & Gibbs, G.V. (1973): The crystal structure and bonding of fluor-tremolite: a comparison with hydroxyl tremolite. *Am. Mineral.* **58**, 879-888.

———, Sueno, S., Papike, J.J. & Prewitt, C.T. (1983): High temperature crystal chemistry of K and Na fluor-richterites. *Am. Mineral.* **68**, 924-943.

Cromer, D.T. & Liberman, D. (1970): Relativistic calculation of anomalous scattering factors for X rays. *J. Chem. Phys.* **53**, 1891-1898.

——— & Mann, J.B. (1968): X-ray scattering factors computed from numerical Hartree–Fock wave functions. *Acta. Crystallogr.* **A24**, 321-324.

Docka, J.A., Post, J.E., Bish, D.L. & Burnham, C.W. (1987): Positional disorder of the A-site cations in *C2/m* amphiboles. Model energy calculations and probability studies. *Am. Mineral.* **72**, 949-958.

Gibbs, G.V. (1966): Untitled article. In *AGI Short Course Lecture Notes on Chain Silicates*, 1-23.

——— & Prewitt, C.T. (1968): Amphibole cation site disorder. *Int. Mineral. Assoc., Proc., Fifth Gen. Meet.* (Cambridge, 1966). (abstr.).

Graham, C.M. & Navrotsky, A. (1986): Thermochemistry of the tremolite – edenite amphiboles using fluorine analogues, and applications to amphibole – plagioclase – quartz equilibria. *Contrib. Mineral. Petrol.* **93**, 18-32.

Greenwood, H.J. (1979): Thermodynamic properties of edenite. *Geol. Surv. Can., Pap.* **79-1B**, 365-370.

Hawthorne, F.C. (1983): The crystal chemistry of the amphiboles. *Can. Mineral.* **21**, 173-480.

——— & Grundy, H.D. (1972): Positional disorder in the A-site of clino-amphiboles. *Nature Phys. Sci.* **235**, 72-73.

——— & ——— (1973a): The crystal chemistry of the amphiboles. I. Refinement of the crystal structure of ferrotschermakite. *Mineral. Mag.* **39**, 36-48.

——— & ——— (1973b): The crystal chemistry of the amphiboles. II. Refinement of the crystal structure of oxy-kaersutite. *Mineral. Mag.* **39**, 390-400.

——— & ——— (1977): The crystal chemistry of the amphiboles. III. Refinement of the crystal structure of a subsilicic hastingsite. *Mineral. Mag.* **41**, 43-50.

——— & ——— (1978): The crystal chemistry of the amphiboles. VII. The crystal structure and site chemistry of potassian ferri-taramite. *Can. Mineral.* **16**, 53-62.

Heritsch, H. (1955): Bemerkungen zur Schreibung der kristallchemischen Formel der Hornblende. *Tschermaks Mineral. Petrogr. Mitt.* **5**, 242-245.

Hinrichsen, T. & Schürmann, K. (1977): Experimental investigations on the Na/K substitution in edenites and pargasites. *Neues Jahrb. Mineral. Abh.* **130**, 12-18.

Na, K.C., McCauley, M.L., Crisp, J.A. & Ernst, W.G. (1986): Phase relations to 3 kbar in the systems edenite + H_2O and edenite + excess quartz + H_2O. *Lithos* **19**, 153-163.

OBERTI, R., UNGARETTI, L., CANNILLO, E. & HAWTHORNE, F.C. (1992): The behaviour of Ti in amphiboles. I. Four- and six-coordinated Ti in richterite. *Eur. J. Mineral.* **4**, 425-439.

PAPIKE, J.J., ROSS, M. & CLARK, J.R. (1969): Crystal-chemical characterization of clinoamphiboles based on five new structure refinements. *Mineral. Soc. Am., Spec. Pap.* **2**, 117-136.

PREWITT, C.T. (1963): Crystal structures of two synthetic amphiboles. *Geol. Soc. Am., Spec. Pap.* **76**, 132-133 (abstr.).

RAUDSEPP, M., TURNOCK, A.C. & HAWTHORNE, F.C. (1991): Amphibole synthesis at low pressure: what grows and what doesn't. *Eur. J. Mineral.* **3**, 983-1004.

SHANNON, R.D. (1976): Revised effective ionic radii and systematic studies of interatomic distances in halides and chalcogenides. *Acta Crystallogr.* **A32**, 751-767.

UNGARETTI, L. (1980): Recent developments in X-ray single crystal diffractometry applied to the crystal-chemical study of amphiboles. *God. Jugosl. Cent. Kristalogr.* **15**, 29-65.

———, SMITH, D.C. & ROSSI, G. (1981): Crystal-chemistry by X-ray structure refinement and electron microprobe analysis of a series of sodic-calcic to alkali amphiboles from the Nybö eclogite pod, Norway. *Bull. Minéral.* **104**, 400-412.

WIDMARK, E.T. (1974): An edenite-forming reaction: hydrothermal experiments. *Neues Jahrb. Mineral., Monatsh.*, 323-329.

Received April 24, 1992, revised manuscript accepted April 27, 1993.